

Analysis of Polyhedron Approximated Reflector Antennas

Eiji HANAYAMA and Tadashi TAKANO

The Institute of Space and Astronautical Science
3-1-1 Yoshino-dai, Sagamihara, 229 Japan

1 Introduction

A large deployable antenna possibly adopts a polyhedron approximated reflector which is composed of many flat planes or facets. To analyze radiation characteristics of such antennas, previous works use aperture integration (AI) method with approximate ray tracing to calculate aperture field distribution ^{(1),(2)}. There has been, however, no discussion in regard to its accuracy in comparison with the analytical results without approximation such as the current distribution (CD) method.

For smooth parabolic reflector antennas, the applications of the both methods have already been studied. AI method assures better accuracy for a larger diameter antenna. The approximation degradation of AI method is probable, since the polyhedron approximated reflector is divided into the small facets. This paper analyzes the polyhedron approximated reflector antenna using AI and CD methods. Effects due to the approximation and the application limit of AI method are clarified as a result.

2 Antenna structure

The structure of the polyhedron approximated reflector antenna is shown in Fig. 1. The reflector consists of many triangular facets attached onto paraboloid. The facets projected on the reflector aperture are identical regular triangles which divide the reflector radius by N . The shape of the aperture is regular hexagon of $D/2$ side length, where D is the aperture diameter. The focal length of the prototype paraboloid is represented by F .

Let the origin O be the antenna vertex and let the z -axis be in the direction of the antenna axis. A polar coordinate to express x - y plane is indicated by (ρ, θ) . Simple geometrical calculation gives mechanical reflector error Δz measured in the direction of the antenna axis by Eq. (1).

$$\Delta z = \frac{1}{4F} \left[\frac{D^2}{12N^2} - (x - x_G)^2 - (y - y_G)^2 \right], \quad (1)$$

where (x_G, y_G) represent the coordinates of the gravity center of the facet.

3 Aperture integration method

The aperture integration method with approximation is used to analyze polyhedron approximated reflector antennas. To determine the field distribution on the aperture, the approximate ray tracing is used on the basis of following assumptions.

1. The propagation direction of the rays is parallel with the antenna axis.

2. The amplitude distribution A on the aperture is identical with that of the prototype antenna.
3. The phase distribution Ψ on the aperture can be obtained as the sum of phase error $\Delta\varepsilon$ due to the mechanical error in Eq. (1) and the phase of primary radiated field. The phase error $\Delta\varepsilon$ is expressed by

$$\Delta\varepsilon = \frac{2k\Delta z}{1 + (\rho/2F)^2}, \quad (2)$$

where $k (= 2\pi/\lambda)$ is a wavenumber in free space.

4. The polarization does not change by reflection on the facet.

The primary feed in conjunction with reflectors is supposed to produce uniform field and x -polarized on the aperture. The diameter D , wavelength λ and F/D are supposed 0.6m, 11.88mm and 0.25, respectively. Figure 2 shows the field distribution in the direction $\theta = 0^\circ$ on the aperture at $z = D^2/16F$ using the approximate ray tracing. The amplitude distribution is uniform and the phase distribution is changing periodically with a period of $2u$: the side length of the facet, in accordance with Eqs. (1) and (2).

The rigorous ray tracing does not use the assumptions 1. to 3. and the phase distribution is derived from rigorous pathlength. The rays spread out of the physical facets and overlap each other as a result of the rigorous ray tracing as shown in Fig. 3.

From the aperture field distribution $Ae^{-j\Psi}$, the radiation field E can be obtained by

$$E = \frac{1}{4\pi} \int_S A e^{-j\Psi} \frac{e^{-jk|\mathbf{r}_1|}}{|\mathbf{r}_1|} \left[\left(jk + \frac{1}{|\mathbf{r}_1|} \right) \mathbf{n} \cdot \frac{\mathbf{r}_1}{|\mathbf{r}_1|} + jk\mathbf{n} \cdot \mathbf{s} \right] dS, \quad (3)$$

where \mathbf{r}_1 is the position vector of an observation point with respect to the point on the aperture, \mathbf{n} is a unit vector normal to the aperture and S is the area of the aperture. \mathbf{s} is the unit vector in the direction of a ray at given point on the aperture, and is expressed by

$$\mathbf{s} = \left(\frac{1}{k} \frac{\partial \Psi}{\partial x}, \frac{1}{k} \frac{\partial \Psi}{\partial y}, (1 - s_x^2 - s_y^2)^{1/2} \right). \quad (4)$$

Equations (3) and (4) are valid even in the near field.

4 Current distribution method

The radiation field \mathbf{E} in the current distribution method is expressed by

$$\mathbf{E} = \int_{S'} \{ -j\omega\mu \mathbf{J}_s G - (j/\omega\epsilon) \mathbf{J}_s \cdot \nabla' \nabla' G \} dS', \quad (5)$$

where G is Green's function: $G = \exp(-jk|\mathbf{r} - \mathbf{r}'|)/4\pi|\mathbf{r} - \mathbf{r}'|$, \mathbf{r} and \mathbf{r}' are the position vectors of an observation point and a point on the reflector surface, respectively. S' is the area of the reflector surface. And ω is an angular frequency, and ϵ and μ are the permittivity and the permeability of the free space, respectively.

Reflection's law is assumed to be locally applied on each facet. The induced current density \mathbf{J}_s on the facets is obtained by

$$\mathbf{J}_s = 2\mathbf{n}' \times \mathbf{H}_i, \quad (6)$$

where \mathbf{n}' is a unit vector normal to the facets and \mathbf{H}_i is the incident magnetic field. In CD method, the rigorous field distribution is calculated on the basis of reflector geometry.

Antenna parameters are the same as in the case of AI method. Figure 4 shows the field distribution in the direction $\theta = 0^\circ$ on the aperture using CD method. The field distribution is changing periodically with a period of the side length of the facet. The interference of rays reflected on neighboring facets produces the sinusoidal pattern of amplitude which is maximized at joints of the facets.

5 Calculation results and discussions

In case of $F/D = 0.25$ and $N = 5$, the radiation patterns are calculated by Eqs. (3) and (5) as shown in Fig. 5. It turns out that AI and CD methods are in good agreement. The antenna gains are calculated using both methods for various F , D , λ and N . If the maximum mechanical error is a wavelength λ , the difference of gain values which are derived from two methods becomes 0.1dB.

Though the field distributions using two methods differ from each other as in Figs. 2 and 4, both far field characteristics coincide with each other. In order to investigate this phenomena, the field distribution on various planes is calculated using AI method on the basis of the field distribution on the aperture.

Figure 6 compares the amplitude distributions on the plane at $z = D^2/8F$ using AI method and on the aperture at $z = D^2/16F$ using CD method, respectively. Two distributions coincide with each other. The phase distributions also show good coincidence. It can be said that there is an equivalent relation between the two planes for both methods. Good coincidence of the both far field characteristics in Fig. 5, therefore, is quite agreeable.

From our experimental study, the validity of AI method with approximation was verified ⁽³⁾.

6 Conclusions

For the polyhedron approximated reflector antenna, AI method using approximate ray tracing assures good accuracy, if the maximum mechanical reflector error is smaller than a wavelength. It is not necessary to consider the effect that the direction of the rays is not parallel with the antenna axis. The amplitude distribution does not change and the phase distribution is derived from mechanical error.

The accurate field distribution on the aperture is obtained using AI method, if the field distribution on the aperture by approximate ray tracing is transformed by AI method into the field distribution on the plane apart by the same distance between the aperture and the antenna vertex.

References

- (1) T. Takano and M. Ui : "A study on reflector error of large deployable antennas and its effects on radiation characteristics", Trans. IEICE., **J71-B**, 6, pp.764-771 (June 1988).
- (2) C. R. Cockrell : "Electromagnetic analysis for surface tolerance effects on large space antennas", Large space antenna systems technology — 1984, NASA CP-2368 part 2, pp.655-673 (Dec. 1984).
- (3) E. Hanayama and T. Takano : "Investigation of radiation characteristics of large deployable antennas using a model antenna", Trans. IEICE. (To be published).

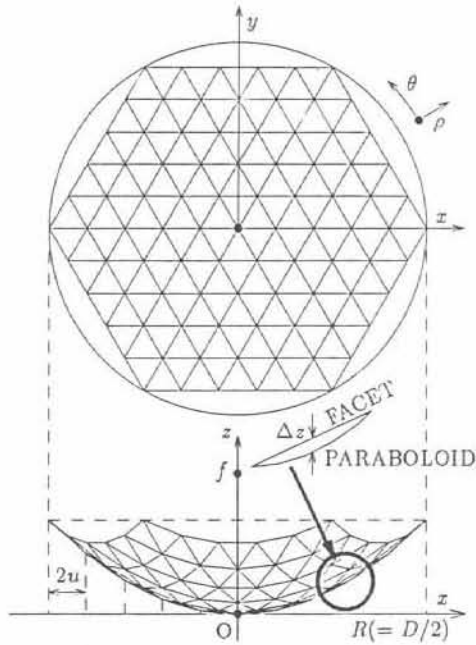


Fig. 1. Structure of the antenna.

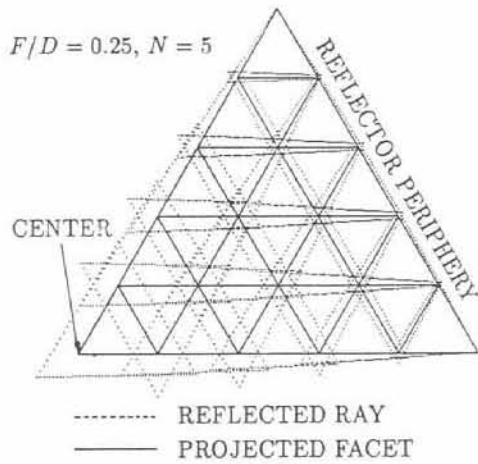


Fig. 3. Spread of ray on the aperture.

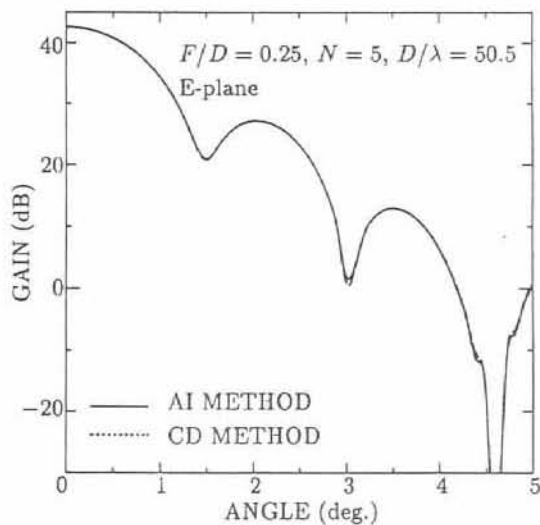


Fig. 5. Radiation patterns of the antenna.

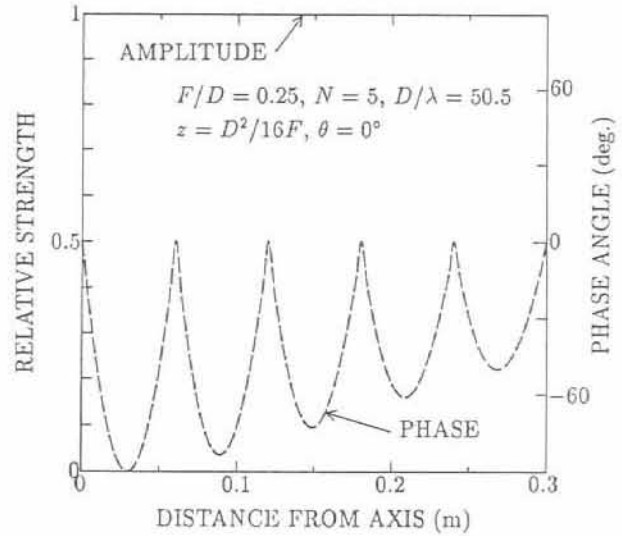


Fig. 2. Field distribution on the aperture using approximate ray tracing.

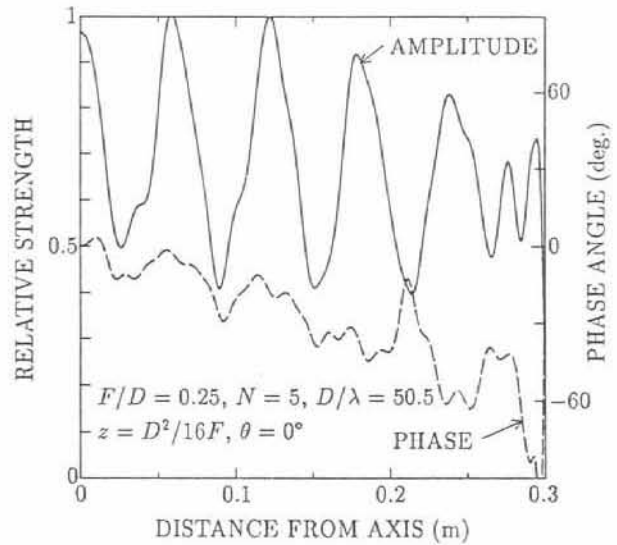


Fig. 4. Field distribution on the aperture using CD method.

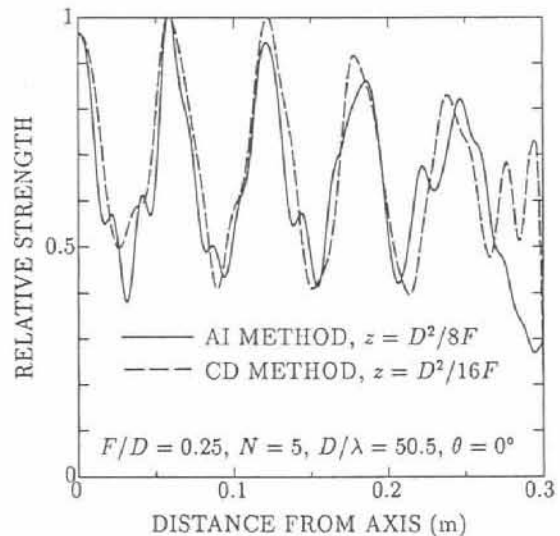


Fig. 6. Comparison of the field distributions.